Predicting aircraft trajectory uncertainties for terminal airspace design evaluation

Zhu, Xinting; Hong, Ning; He, Fang; Lin, Yu; Li, Lishuai; Fu, Xiaowen

DOI
10.1016/j.jairtraman.2023.102473

Publication date
2023

Document Version
Final published version

Published in
Journal of Air Transport Management

Journal of Air Transport Management 113 (2023) 102473

Contents lists available at ScienceDirect

Journal of Air Transport Management

journal homepage: www.elsevier.com/locate/jairtraman

Predicting aircraft trajectory uncertainties for terminal airspace design evaluation

Xinting Zhu [a], Ning Hong [a], Fang He [a,b], Yu Lin [a], Lishuai Li [a,c,*], Xiaowen Fu [d]

[a] School of Data Science, City University of Hong Kong, Hong Kong SAR
[b] School of Aeronautics and Astronautics, Shanghai Jiao Tong University, Shanghai, Hong Kong SAR
[c] Faculty of Aerospace Engineering, TU Delft, Delft, Netherlands
[d] Department of Industrial and Systems Engineering, The Hong Kong Polytechnic University, China

ARTICLE INFO

Keywords:
Air traffic management
Terminal airspace
Trajectory generation
Air traffic flow
Fuel consumption

ABSTRACT

The terminal airspace that surrounds an airport is the area with high flight density and complex structure. Aircraft are asked to follow the standard arrival and departure routes in terminal airspace, yet the actual trajectories may deviate due to air traffic control (ATC) instructions, pilots' decisions, surveillance and flying performance variations, etc. Predicting aircraft trajectories considering such uncertainties plays a crucial role in evaluating a redesign of the standard routes. Traditional simulation approaches for generating aircraft trajectories in a terminal airspace are cumbersome to use as it requires a detailed setup for each new scenario, while most existing data-driven methods can only be used in an airspace with historical trajectories, not applicable to new structure designs or other terminal areas. To fill in gap, in this paper, we develop a new model based on Multilayer Perceptron Neural Network (MLPNN) to predict aircraft trajectories with uncertainties for terminal airspace design evaluations. A key feature of the proposed model is that it is trained on existing standard routes yet it can be applied to new standard routes to generate trajectories. The enabler of the model's transferability is a novel input-and-output construction method for feature representations of raw trajectory data based on domain knowledge, including trajectory reconstruction, feature engineering, and output designing. After the input-and-output construction, a supervised learning model based on MLPNN is built to predict the standard deviations from the extracted features using historical trajectory data of existing standard routes. Once the model is built, trajectories with uncertainty can be simulated, through applying Gaussian distribution and exponential moving average algorithms, even on newly designed standard routes, where no aircraft have flown yet. Subsequently, new terminal airspace designs could be evaluated for their safety, efficiency, and environmental implications based on the simulated trajectories. The proposed model was tested on real-world operational data. Results showed that the model can quantify the characteristics of aircraft trajectories that are transferable across standard routes, and generate trajectories for new standard routes. We also demonstrated the proposed model on evaluating deficiencies on fuel consumption of actual arrival trajectories compared with the designed arrival routes. The generated trajectories showed 23%–37% more fuel consumption on average than the standard arrival routes in the terminal airspace of Hong Kong International Airport, which was validated with actual flight data.

1. Introduction

The terminal airspace that surrounds an airport is the area with high flight density and complex structure. In fact, nearly half of all fatalities, about 49%, occur on approach and landing in terminal airspace from 2009 through 2019 (Boeing Commercial Airplanes, 2020). The changes in airport and its terminal airspace may affect safety, fuel consumption, noise impact, and pollutant impact (M. Z. Li et al., 2018; M. Z. Li and Ryerson, 2017; Rosenow and Fricke, 2019). Therefore, a comprehensive evaluation of terminal airspace designs is essential to support the safe, efficient, and environmental-friendly operations of new airports.

To evaluate the safety, efficiency, and environmental impact of airspace redesign, generating aircraft trajectories considering uncertainties plays a crucial role. In the terminal area, there are standard

* Corresponding author. School of Data Science, City University of Hong Kong, Hong Kong SAR.
E-mail addresses: xt.zhu@my.cityu.edu.hk (X. Zhu), neil.hong@my.cityu.edu.hk (N. Hong), fanghe7-c@my.cityu.edu.hk (F. He), yulin8@cityu.edu.hk (Y. Lin), lishuai.li@cityu.edu.hk (L. Li), xiaowen.fu@polyu.edu.hk (X. Fu).

https://doi.org/10.1016/j.jairtraman.2023.102473
Received 3 October 2021; Received in revised form 7 July 2023; Accepted 30 August 2023
Available online 9 September 2023

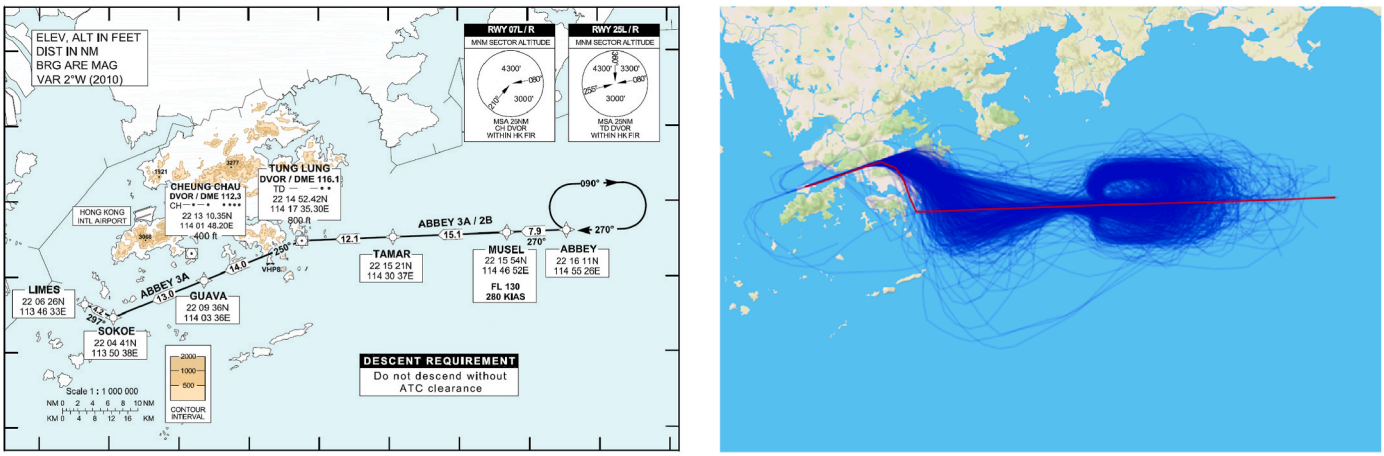

Fig. 1. ABBEY-2B arrival in Hong Kong airspace & the standard route (in red) compared with actual trajectories (in blue).

procedures, such as Standard Instrument Departure routes (SID) and Standard Arrival Routes (STAR). However, actual trajectories may be different from the standard ones, as shown in Fig. 1. Such deviations may be caused by many factors, such as weather conditions, air traffic control (ATC) instructions, pilots' decisions, the performance of aircraft, etc (T. Li and Wan, 2021). Particularly a large amount of trajectory non-conformance happened in terminal airspace come from congestions and flight separation requirements. Even in good weather conditions, there might be many VFR flights, resulting in congestion and trajectory deviations if the airport is not strategically slot constrained (e.g., many US airports). Thus, trajectory generation models to characterize such deviations and predict aircraft trajectories with probabilistic uncertainties are needed as an essential step for the analysis of airspace redesign.

In the field of aviation, there is a vast amount of research related to aircraft trajectory prediction. Most of these studies focus on predicting future aircraft motion for air traffic conflict detection and resolution. These studies account for the uncertainty affecting the aircraft future positions for the avoidance of collision, via a multiple model method (Jilkov et al., 2019; Liu and Hwang, 2011; Yepes et al., 2007), the worst-case approach (Huang and Tomlin, 2009; Tomlin et al., 1998), a Sequential Monte Carlo method (Lymperopoulos and Lygeros, 2010; Visintini et al., 2006), a Hidden Markov Model (Ayhan and Samet, 2016; Seah and Hwang, 2009) and others. These researches focus on quantifying the probability of conflicts between two aircraft or more and perform trajectory prediction for individual aircraft, not for a fleet of aircraft in a particular airspace.

Another line of studies related to trajectory prediction is on the dynamic terminal route concept, developing trajectory models to optimize aircraft movement in terminal airspace (Murça and Müller, 2015). Pfeil developed an A*-based algorithm for the design of three-dimensional (3D) terminal routes under uncertain weather conditions (Pfeil, 2011). Zhou et al. introduce a fast-marching method to generate 3D SIDs and STARs at a strategic level, where a simulated annealing method is used to find the optimal order (Zhou et al., 2014). Sidiropoulos et al. propose a priority-based framework to design dynamic arrival and departure routes for the multi-airport system (Sidiropoulos et al., 2018). These methods aim at designing new routes but not quantifying the uncertainties of flying existed routes.

Traditional methods for evaluating new designs of arrival/departure routes in a terminal airspace are simulation-based. Several simulation models and products are available, including the Terminal Area Route Generation and Traffic Simulation (TARGETS) developed by MITRE (CSSI Inc.; MITRE, 2021) and the Future ATM Concept Evaluation Tool (FACET) (Bilimoria et al., 2001) developed by NASA Ames Research Center. However, these simulation tools either require intensive inputs or human-in-the-loop setup to obtain the uncertainties involved with flying the standard routes, or lack of the capability to simulate the uncertainties.

Recent efforts have been made to train a statistical or machine learning model on historical surveillance data directly, to capture non-deterministic influences for aircraft trajectory prediction(Bongiorno et al., 2017). One important branch is studying flight historical data by regression analysis, such as a multiple linear regression (S. Hong and Lee, 2015), a functional regression (Tastambekov et al., 2014), a local polynomial regression (Hamed et al., 2013), a stepwise regression (de Leege et al., 2013), and neural networks (Alligier et al., 2015; Khan et al., 2021). These approaches have returned successful outcomes for improving the trajectory prediction accuracy. Another branch involves clustering turning points or clustering historical aircraft trajectories in terminal airspace (Barratt et al., 2018; Gariel et al., 2011; Jarry et al., 2020; Mahboubi and Kochenderfer, 2017; Marzuoli et al., 2014; Murça et al., 2020; Murca and Hansman, 2019; Olive and Morio, 2019; Ren and Li, 2018). However, a common limitation of these methods is that they can only be used on existing standard routes of the current airport where historical trajectory data are available, while they cannot be applied to routes under design, terminal airspace with new structures, or other airports.

To fill this gap in trajectory generation, we develop a novel machine learning model for predicting aircraft trajectory uncertainties in a terminal airspace with new route structures. The primary idea of our proposed method is to extract features that could be generalized for different route structures from the historical surveillance data. The proposed model can capture statistical properties of the aircraft trajectory uncertainty in a terminal airspace. The main advantage of our model compared with existing methods is that it is transferable to new standard routes. By introducing a trajectory reconstruction procedure, the features are re-constructed from raw trajectory data and the features are universal to different route structures.

This paper is structured as follows: The proposed framework is described in Section 2. Model evaluation and testing are presented in Section 3. In Section 3, we also apply the proposed approach for fuel consumption evaluation in the terminal airspace of Hong Kong International Airport. Finally, conclusions and future works are presented in Section 4.

2. Methodology

We propose a machine learning approach to model the uncertainty of aircraft trajectories in terminal airspace and generate trajectories for terminal airspace redesign analysis. The model, referred as Trajectory Generation Model in this paper, predicts the deviations of actual aircraft

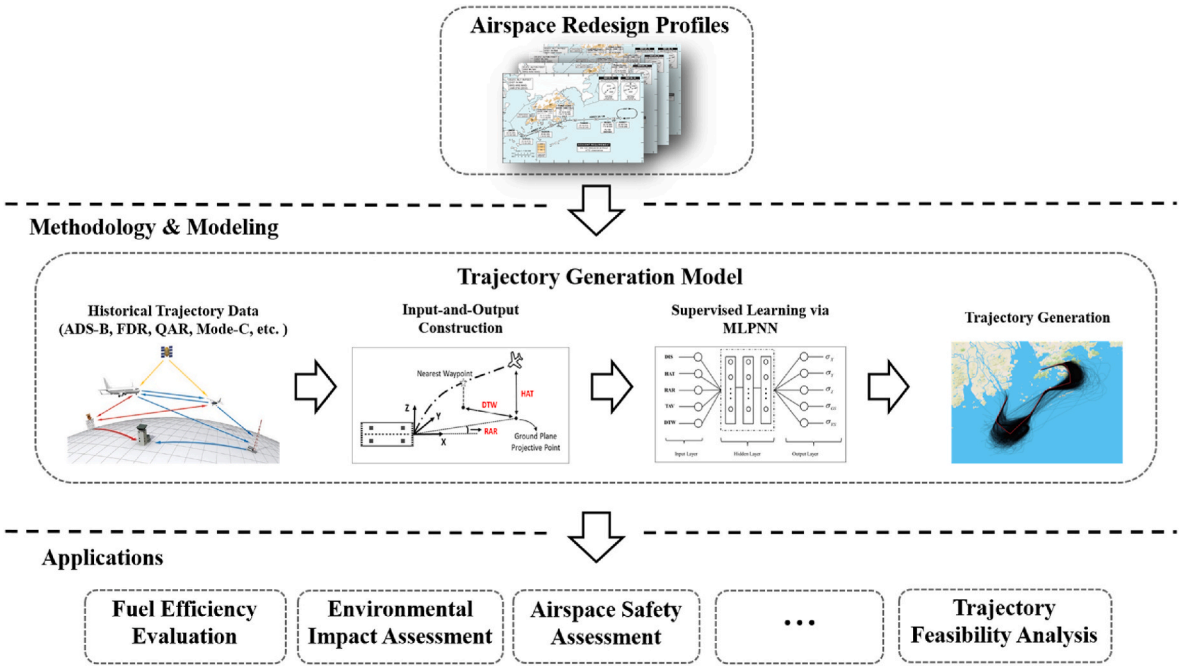

Fig. 2. Illustration of terminal airspace redesign assessment process.

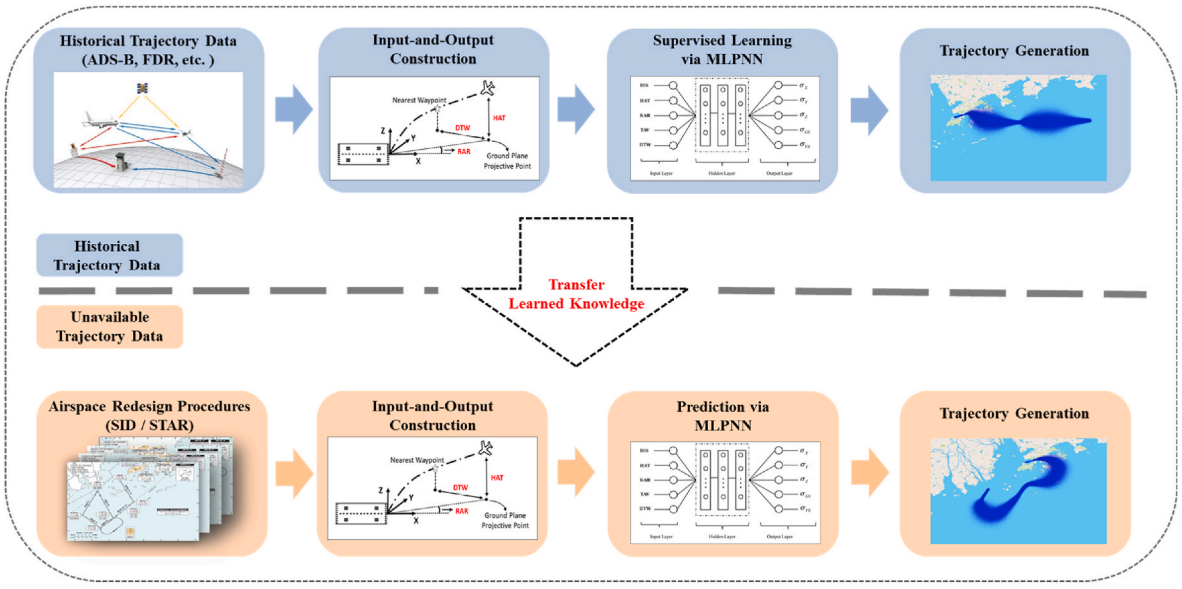

Fig. 3. The framework of the trajectory generation model.

trajectories from the designed routes. The simulated trajectories generated model can then be used for a number of analysis, e.g. fuel efficiency evaluation, environmental impact assessment, airspace safety assessment, etc., as illustrated in Fig. 2.

The model uses a transfer learning approach, training on existing standard routes but can be applied to new standard routes for trajectory generation. The inputs of the model are historical trajectory data and existing standard arrival/departure routes. Then, the uncertainty of trajectories relative to standard routes is characterized and parametrized via the input-and-output construction step and the supervised learning via MLPNN step. Lastly, when a new design of standard routes is given, the model can simulate aircraft trajectories flying these newly designed routes, with probabilistic uncertainties on a system level.

Overall, three modules are included in the proposed model: 1) input-and-output construction, 2) supervised learning via MLPNN, and 3) trajectory generation, as illustrated in Fig. 3. In this paper, we demonstrate how this model can be used for fuel consumption analysis, as an example of the follow-up evaluation analysis. The details are provided in the following sub-sections.

1. Input-and-Output Construction

A key challenge of such a model lies in how to make it adaptable on different terminal airspace routes and airports. Airports vary in size, layout, runway configuration, etc., and the corresponding terminal airspace structures differ as well. If a learning model is directly trained on raw trajectory data, it won't be applicable to new standard routes or new airports where trajectory data are not available yet. Therefore, the

Table 1
The right-handed cartesian coordinate systems for each runway.

The Origin	The Positive Orientation of Axis		Unit
Threshold position of the runway	X-axis:	The opposite direction of the runway	m
	Y-axis:	Rotating X-axis 90° counterclockwise	m
	Z-axis:	Vertically upward	m

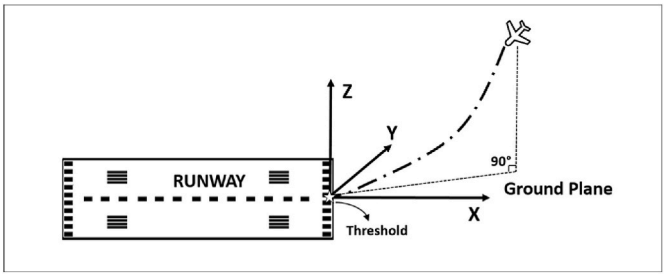

Fig. 4. The framework of the trajectory generation model.

Table 2
Five key informative features for supervised learning.

Inputs	Description	Unit
DIS	Accumulated horizontal flying distance to the runway threshold	m
ALT	Relative altitude above the touchdown zone, namely Z	m
RAR	Relative angle to the positive X-axis	rad
TAV	Track angle variation between adjacent data points	rad
DTW	Horizontal distance to nearest waypoint from STAR profiles	m

Input-and-Output Construction module is developed to reconstruct trajectory data into designated features that capture the underlying patterns of uncertainties relative to the standard routes, so that these features could be easily adapted to other airports to test different procedures. This module includes a unified method to process original ungraded data to standard trajectory data of high quality, extract key features to be used as model inputs, and to design the outputs for subsequent supervised learning. There are three submodules: a) Trajectory Reconstruction, b) Feature Engineering, and c) Output designing in the Input-and-Output Construction.

1. Trajectory Reconstruction

To make our model a general approach, that can be trained by different data sources and applied in various terminal airspace, we firstly conduct the trajectory reconstruction. Trajectory reconstruction is the process of processing original ungraded data into standard trajectory data of high quality. The Automatic Dependent Surveillance-Broadcast (ADS-B) data is selected as the data source of the aircraft trajectory prediction model. Each ADS-B data record we collected contains.

1. Type of operation (departure/arrival),
2. Aircraft number,
3. Coordinated Universal Time (UTC) timestamp t,
4. Position information, longitude P_x, latitude P_y, and altitude P_z,
5. Track ψ,
6. Ground speed V_h,
7. Vertical velocity V_v.

Each record with the same aircraft number belongs to an aircraft j, and the group of all records for that aircraft forms the trajectory T_l, $l = 1,\ldots,n$, where n is the total number of trajectories in the dataset.

There are three main complications with the trajectories in their original format. First, the raw trajectories are specific to each runway. Features directly extracted from the raw data would be meaningful for other runways, standard routes, or airports. Second, the trajectories may contain outliers or noises. Third, the trajectories are not of equal length.

We tackle the second complication first as it is a simple data filtering process. We use the exponential moving average (EMA) algorithm (Wang et al., 2018) to smooth trajectory data, acting as low-pass filters to remove high-frequency noise. Despite its simplicity, it is highly competitive with other more sophisticated trajectory smoothing methods. The simplest form of exponential smoothing is given by the formula (Chazal et al., 2011),

$$P_i^{'} = \begin{cases} P_1, i = 1 \\ \alpha P_i + (1-\alpha)\cdot P_{i-1}^{'}, i > 1 \end{cases} \quad (1)$$

where, α represents the degree of weighting decrease, which is a constant smoothing factor between 0 and 1. P_i denotes one of the aircraft 3D position variables (P_x, P_y, P_z) at the data point i and $P_i^{'}$ is the value after smoothing by EMA at the data point i.

Then, to solve the second complication, we build new Cartesian coordinate systems in each runway to transform position data into coordinates that are universal to any runway, as illustrated in Table 1 and Fig. 4. According to the landing slot of the aircraft, its 3D position information (P_x, P_y, P_z) could be transformed into (X, Y, Z) in corresponding runway coordinate system. After transformation, we calculate the value of accumulated horizontal distance to the runway threshold, which is defined as DIS. Then, we deal with the varying length issue by distance aligning based on DIS. We set the first data point as the landing site of aircraft, and select 150 nautical miles (NM) DIS backward for the trajectory. We set a data point at each 3 NM interval so that all trajectories have the length of 51 data points. Trajectories that are significantly shorter than 150 NM are discarded. Then, trajectories that are shorter than 150 NM are extrapolated and trajectories that are longer than 150 NM are truncated. Meanwhile, the parameters of ADS-B data, such as track ψ, ground speed V_h, and vertical velocity V_v, are obtained in each data points through linear interpolation.

The reconstructed trajectories have the same length after distance-aligning processing, which includes recomputed parameters: 3D position information (X, Y, Z), track ψ, ground speed V_h, and vertical velocity V_v.

2. Feature Engineering

Based on domain knowledge of air traffic control and flight operations, we engineered five key features from the reconstructed trajectory data, which describes the relative position of aircraft in reference to the standard route. These five key features, as illustrated in Table 2 and Fig. 5, are derived based on the reconstruction trajectory data and STAR profiles. The 'DIS' is the aircraft's accumulated horizontal flying distance from its position to the runway threshold, and it could be obtained from the position data (X, Y, Z). The 'ALT', namely Z, means the relative altitude above the touchdown zone. The 'RAR' is defined as the relative angle to X-axis in the right-handed coordinate system and its range is $(-\pi, \pi]$. We assume angles on the coordinate plane have an initial side on the positive X-axis, and the terminal side of the angle is the side where the ground plane projective point of aircraft located. Positive angles on the coordinate plane are angles that go in a counterclockwise direction, while negative angles on the coordinate plane are angles that go in a clockwise direction. The 'TAV' represents the track angle variation between adjacent data points. The first data point is the landing site of aircraft, and its 'TAV' is set to 0 rad. By deductive calculation backward step-by-step, it's simple to derive 'TAV' values for the other data points based on the parameter track ψ. The 'DTW' refers to the horizontal distance to the nearest waypoint from STAR profiles. For each data

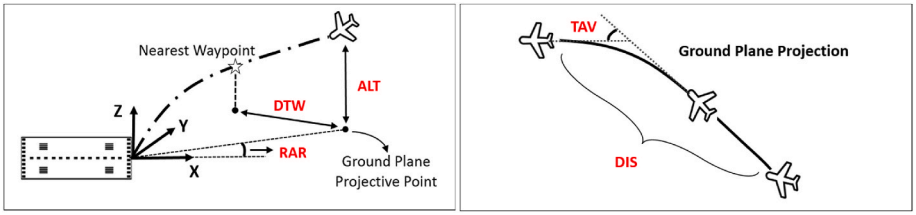

Fig. 5. Five key informative features for supervised learning.

Table 3
Five output variables designed for supervised learning.

Outputs	Description	Unit
σ_X	The standard deviation of the recomputed parameter X	m
σ_Y	The standard deviation of the recomputed parameter Y	m
σ_Z	The standard deviation of the recomputed parameter Z	m
σ_{GS}	The standard deviation of the recomputed ground speed V_h	m/s
σ_{VS}	The standard deviation of the recomputed vertical velocity V_v	m/s

point, we calculate the horizontal distance between the aircraft and all waypoints from the relevant STAR profile, and the minimum value is the target value.

In summary, each data point in the reconstruction trajectory now contains five key informative features, namely DIS, ALT, RAR, TAV, and DTW, which are underlying attributes of the flight trajectory, relative to the standard route.

3. Output Designing

As for target outputs for the supervised learning in the next module, we use standard deviations to summarize the uncertainties of trajectories, as depicted in Table 3 and Fig. 6, which include 3D position information (X, Y, Z), ground speed V_h, and vertical velocity V_v, in the reconstructed trajectory data.

To summarize, each data point now contains five key informative features (DIS, ALT, RAR, TAV, and DTW) as inputs, and five output variables (σ_X, σ_Y, σ_Z, σ_{GS} and σ_{VS}) designed for supervised learning.

2. Supervised Learning via MLPNN

After accomplishing the input-and-output construction, the next step is to develop the MLPNN model to predict designed outputs, based on the key informative features extracted from the reconstruction trajectory data and STAR (or SID) profiles. MLPNN is one of the most commonly used artificial neural network. In this study, MLPNN is tested against a few other advanced regression methods, which are support vector regression (SVR), Random Forest (RF), and Gaussian process regression (GPR). Details on the performance comparison of different regression methods can be found in Section 3.3.

Here, we provide a brief introduction of the MLPNN model used in the paper. MLPNN normally consists of three sequential layers: input layer, hidden layer, and output layer. In this study, each input vector is $x_i = [DIS, ALT, RAR, TAV, DTW]$, which is a set of underlying attributes related to the flight trajectory. Further, each output vector $o_i = [\sigma_X, \sigma_Y, \sigma_Z, \sigma_{GS}, \sigma_{VS}]$, is a set of standard deviations of 3D position information and aircraft velocity information. The structure of MLPNN employed for the standard deviation prediction is shown in Fig. 7. The goal of the MLPNN model is to develop a neural network that can accurately predict the standard deviations based on the input features of future data, by updating the weights in the network from the errors calculated of each training. For each neuron j in the hidden layer, it would sum up its input signals x_i, after multiplying them by their respective connection weights w_{ji}. The output of each neuron is described as follows:

$$y_j = f\left(\sum w_{ji} x_i + b\right) \tag{2}$$

where, b is a bias term and f is an activation function. The commonly used activation functions include the sigmoid function, the hyperbolic tangent, or a Rectified Linear Unit (ReLu) (Nair and Hinton, 2010).

During the training process, the weight w_{ji} is adjusted to minimize the differences between the desired and actual values of the output neurons. The minimization objective function is defined as,

$$E = \frac{1}{2}\sum_j \left(y_{dj} - y_j\right)^2 \tag{3}$$

where, y_{dj} is the desired value and y_j is the actual value of the output for

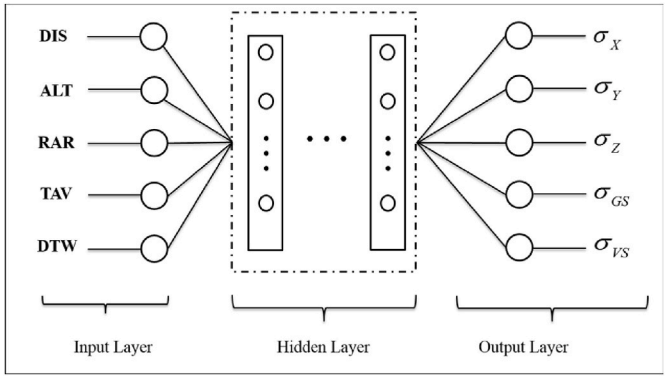

Fig. 7. The structure of MLPNN employed for the standard deviations prediction.

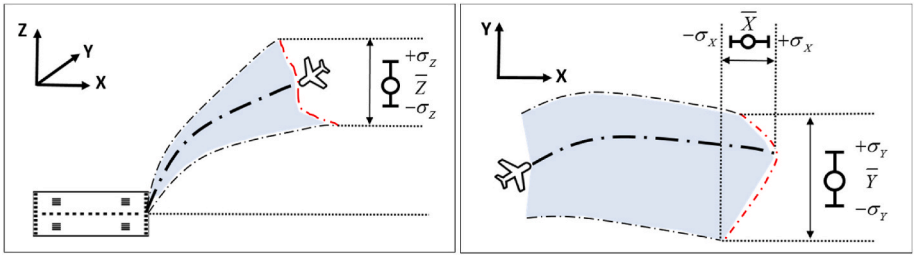

Fig. 6. The standard deviation of recomputed 3D position information (*X, Y, Z*).

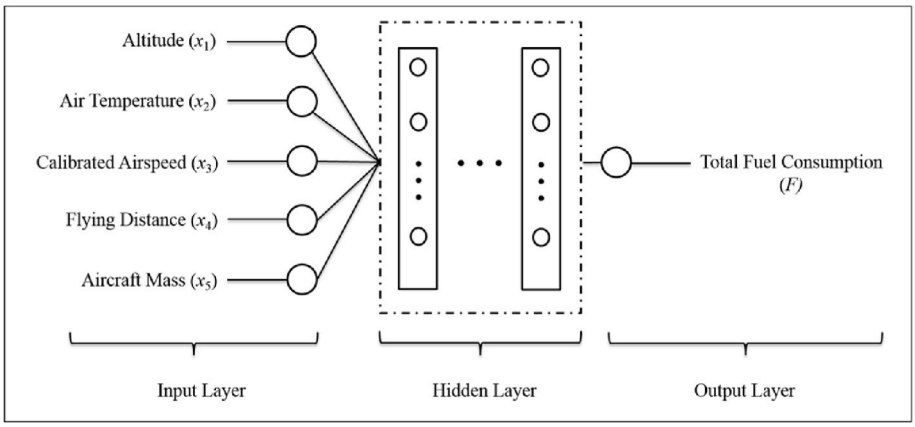

Fig. 8. Fuel consumption estimation model for terminal airspace redesigns.

Table 4
Feature extraction for inputs of fuel consumption estimation model.

Target Inputs	Description of Feature Extraction
Flying Distance	Calculate from position variables X' and Y' of simulated trajectories
Altitude	Calculate from position variable Z' of simulation trajectories
Air Temperature	Obtain from METARs data
Calibrated Airspeed	Calculate from speed variable V_h' of simulation trajectories
Aircraft Mass	Use the values from the manufacturers or FDR data directly

the neuron j.

3. Trajectory Generation

In the last module, we develop a method to simulate aircraft trajectories based on the output of the MLPNN module by applying Gaussian distribution and exponential moving average algorithms. The MLPNN trained in the previous step is not specific to a STAR. It can be transferred directly to another STAR and simulate its associated trajectories considering uncertainty. We apply a Gaussian distribution to simulate trajectories when given a new STAR in terminal airspace. First, we translate the new STAR into the five features as specified in Module I. Next, we use the trained MLPNN to obtain the five standard deviations. Lastly, we randomly generate the 3D position information (X, Y, Z), ground speed V_h, and vertical velocity V_v according to five Gaussian distributions. These five Gaussian distributions have means, $\mu_i = (X_i, Y_i, Z_i, V_{hi}, V_{vi})$, based on the new STAR, and standard deviations, $\sigma_i = (\sigma_{Xi}, \sigma_{Yi}, \sigma_{Zi}, \sigma_{GSi}, \sigma_{VSi})$, calculated from the MLPNN module. The notations and the probability density functions (PDF) of these five simulated parameters in data point i on a trajectory are formulated as,

$$X_i^{'} \sim N(X_i, \sigma_{Xi}); PDF \Rightarrow f(a) = \frac{1}{\sigma_{Xi}\sqrt{2\pi}} e^{\frac{-(a-X_i)^2}{2\sigma_{Xi}^2}} \tag{4}$$

$$Y_i^{'} \sim N(Y_i, \sigma_{Yi}); PDF \Rightarrow f(b) = \frac{1}{\sigma_{Yi}\sqrt{2\pi}} e^{\frac{-(b-Y_i)^2}{2\sigma_{Yi}^2}} \tag{5}$$

$$Z_i^{'} \sim N(Z_i, \sigma_{Zi}); PDF \Rightarrow f(c) = \frac{1}{\sigma_{Zi}\sqrt{2\pi}} e^{\frac{-(c-Z_i)^2}{2\sigma_{Zi}^2}} \tag{6}$$

Table 5
ADS-B data description.

Data	Target Flights	Time	Number of Flights	Sample Frequency
ADS-B	Landing at HKIA	January, May, and June in 2018	30,798	60 Hz

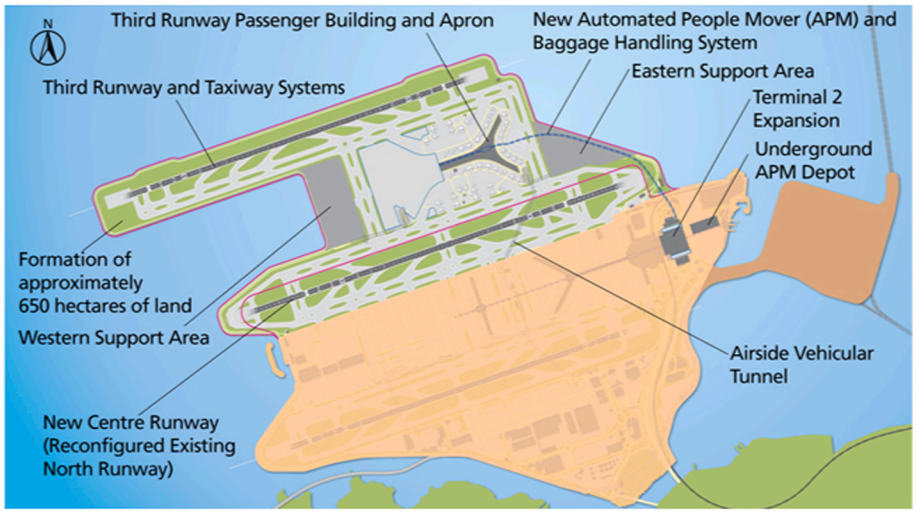

Fig. 9. Tentative layout of the three-runway system at HKIA.

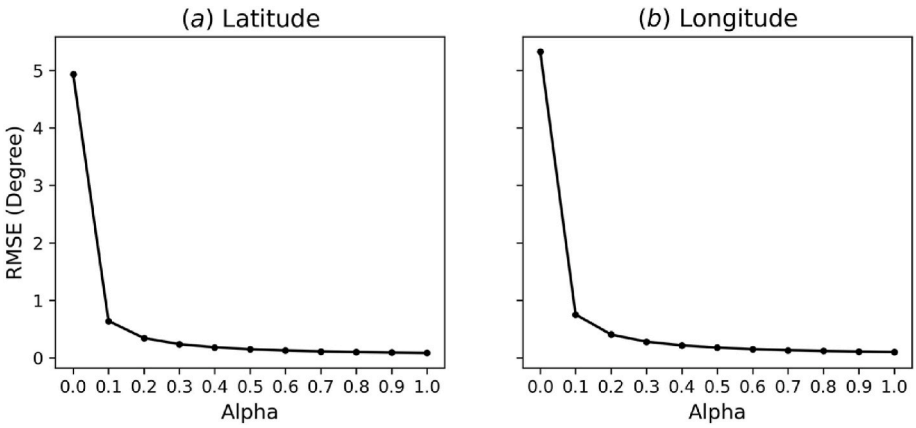

Fig. 10. Sensitive analysis of smoothing factor α.

Fig. 11. Coordinate system transformation for HKIA.

Table 6
Overview of ADS-B data after input-and-output construction.

Number of Trajectories	Data Points for Each Trajectory	Number of Datasets	Inputs of Datasets	Outputs of Datasets
30,798	51	1570698	$(DIS, ALT, RAR, TAV, DTW)$	$(\sigma_X, \sigma_Y, \sigma_Z, \sigma_{GS}, \sigma_{VS})$

$$V_h^{'}i \sim N(V_{hi}, \sigma_{GSi}); PDF \Rightarrow f(d) = \frac{1}{\sigma_{GSi}\sqrt{2\pi}} e^{\frac{-(d-V_{hi})^2}{2\sigma_{GS}^2 i}} \tag{7}$$

$$V_v^{'}i \sim N(V_{vi}, \sigma_{VSi}); PDF \Rightarrow f(e) = \frac{1}{\sigma_{VSi}\sqrt{2\pi}} e^{\frac{-(e-V_{vi})^2}{2\sigma_{VS}^2 i}} \tag{8}$$

Based on the PDFs, we can create five normally distributed sets of random numbers of $(X_i^{'}, Y_i^{'}, Z_i^{'}, V_h^{'}i, V_v^{'}i)$ for each data point, and then generate new trajectories by making connections of these simulated points $(X_i^{'}, Y_i^{'}, Z_i^{'})$ in order of data point sequencing number i.

After simulating new trajectories, we do trajectory smoothing for the rationality of track angle variation using the EMA algorithm. The form of exponential smoothing for a simulated trajectory is given by the formulas,

$$S_i = \begin{cases} X_1^{'}, i = 1 \\ \beta X_i^{'} + (1-\beta)\cdot S_{i-1}, i > 1 \end{cases} \tag{9}$$

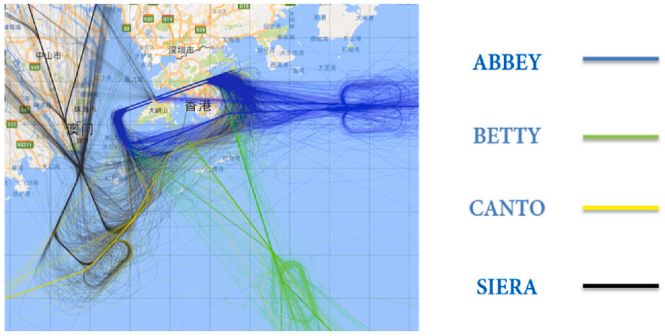

Fig. 12. Four types of arrival routes in Hong Kong terminal airspace.

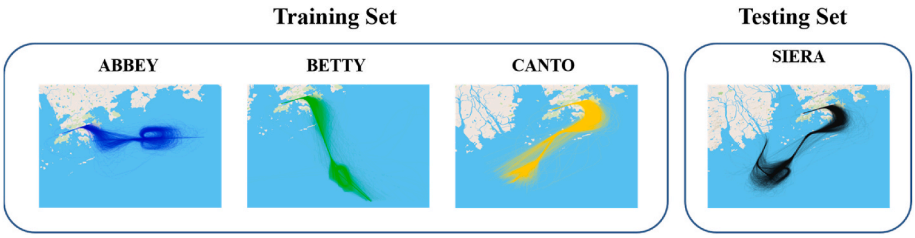

Fig. 13. Training set and testing set for modeling.

Table 7
Detailed setting of the train-test split.

	Training Set			Testing Set
Arrival Routes	ABBEY	BETTY	CANTO	SIERA
Number of Flights	9990	7719	4843	8246
Split Percentage	73%			27%

where, β represents the constant smoothing factor. $X_i^{'}$ is one of the new position variables at the data point i and S_i is the value after smoothing by the EMA at the data point i.

4. Preparation for Airspace Analysis

The trajectories generated from the previous modules are now ready to be used for the following evaluation analysis of airspace designs. Here, to demonstrate how to use the simulated trajectories for a fuel consumption evaluation. The fuel consumption estimation model, as shown in Fig. 8, is for fast assessment of system-level fuel consumption about terminal airspace redesigns, which is proposed by Hong and Li (N. Hong and Li, 2018). The inputs of this model are the aircraft's altitude, the air temperature, the calibrated airspeed, flying distance, and the aircraft mass when descending. Some of these inputs are calculated from the simulated trajectories, while some are obtained from Meteorological Aerodrome Reports (METARs) and other sources. The detailed process is illustrated in Table 4. The output is the fuel burn when flying the simulated trajectories.

3. Evaluation and testing

The Airport Authority Hong Kong plan to expand Hong Kong International Airport (HKIA) into a three-runway system in project Master Plan 2030 by Airport Authority Hong Kong (2011), as shown in Fig. 9. In this context, we demonstrate the proposed trajectory generation model via a case study of HKIA terminal airspace to show how it can be used for fuel efficiency evaluation of airspace designs.

4. Operational data description

The ADS-B dataset used in this study is collected from Flightradar24 every minute for 3 months, namely January, May, and June in 2016, covering all flights landing at HKIA. Each item of the dataset consists of several attributes, which include the flight ID, latitude, longitude, altitude, track, origin airport, destination airport, aircraft type, date, and monitoring time. The ground speed and vertical velocity in our analysis are derived from the position measurements. The data description of the ADS-B dataset is given in Table 5.

2. Input-and-Output Construction of ADS-B data

In this part, the objective is to process ADS-B data to the standard trajectory data of high quality, extract key features as inputs, and finally design the outputs for subsequent supervised learning. We handle the outlier and noise problems by using the EMA algorithm, with the smoothing factor α setting to 0.5 based on testing. The value of smoothing factor is decided by the sensitive analysis as shown in Fig. 10. We calculated the RMSE between raw trajectory and smoothed trajectory as a function of alpha ranging from 0 to 1 with a step of 0.1. Before conducting the trajectory reconstruction, we identify the landing runway in HKIA of each flight based on the position information. Then, we build new Cartesian coordinate systems for each runway, as shown in Fig. 11, to perform the trajectory reconstruction process. The 30,798 reconstructed trajectories all have the same length with 51 data points. Each data point includes recomputed parameters: 3D position information (X, Y, Z), track ψ, ground speed V_h, and vertical velocity V_v. After that, the feature engineering and target outputs designing are executed for supervised learning based on the above-mentioned methods in Section 2.1. The detailed information of processed ADS-B data after input-and-output construction is summarized in Table 6.

After input-and-output construction, the identification of which STAR the flight trajectories belong to is performed. There are four main kinds of STARs, namely ABBEY, BETTY, CANTO, and SIERA, and they are different from each other in terms of trajectory characteristics. We classify the trajectories based on waypoints information from the STARs profiles, and the classification results are shown in Fig. 12. To test the transfer learning capability of our model, we train the model on three

Table 9
Parameter settings for RF, SVR, GPR, and OLS models.

Model	Parameter Settings Description
RF	(i) Number of trees ***n_trees*** $=$ ***100***; (ii) The maximum depth of the tree ***d_max*** $=$ ***11***; (iii) Criterion is '***MSE***'; (iv) The features to consider when splitting ***f_max*** $=$ ***3***
SVR	(i) Kernel used is '***RBF***'; (ii) Kernel coefficient $\gamma =$ ***0.2***; (iii) Regularization parameter ***C*** $=$ ***1***; (iv) Epsilon value $\varepsilon =$ ***0.1***
GPR	(i) Kernel used is '***RBF***'; (ii) Kernel parameters optimizer is '***L-BFGS-B***' algorithm; (iii) Value added to the diagonal of the kernel matrix $\beta = 1e^{-10}$

Table 10
Comparison of model Performance by prediction accuracy.

PA = 1-MAPE	σ_X	σ_Y	σ_Z	σ_{GS}	σ_{VS}
RF	76.42%	81.34%	87.48%	85.94%	87.77%
SVR	80.92%	77.99%	87.49%	82.81%	85.46%
GPR (MEAN)	56.37%	44.52%	70.78%	80.96%	86.17%
MLPNN	**83.63%**	**86.91%**	**91.25%**	**87.99%**	**87.39%**

Table 8
Parameter settings for MLPNN model.

Hidden Layer Sizes	Activation Function	Weight Optimization	Exponential Decay Rate for 'Adam'	L2 Penalty Parameter	Random state value	Mini-batch size
[5, 5, 3]	'ReLU'	'Adam' optimizer	$\beta_1 = 0.9$; $\beta_2 = 0.999$	0.0001	1	64

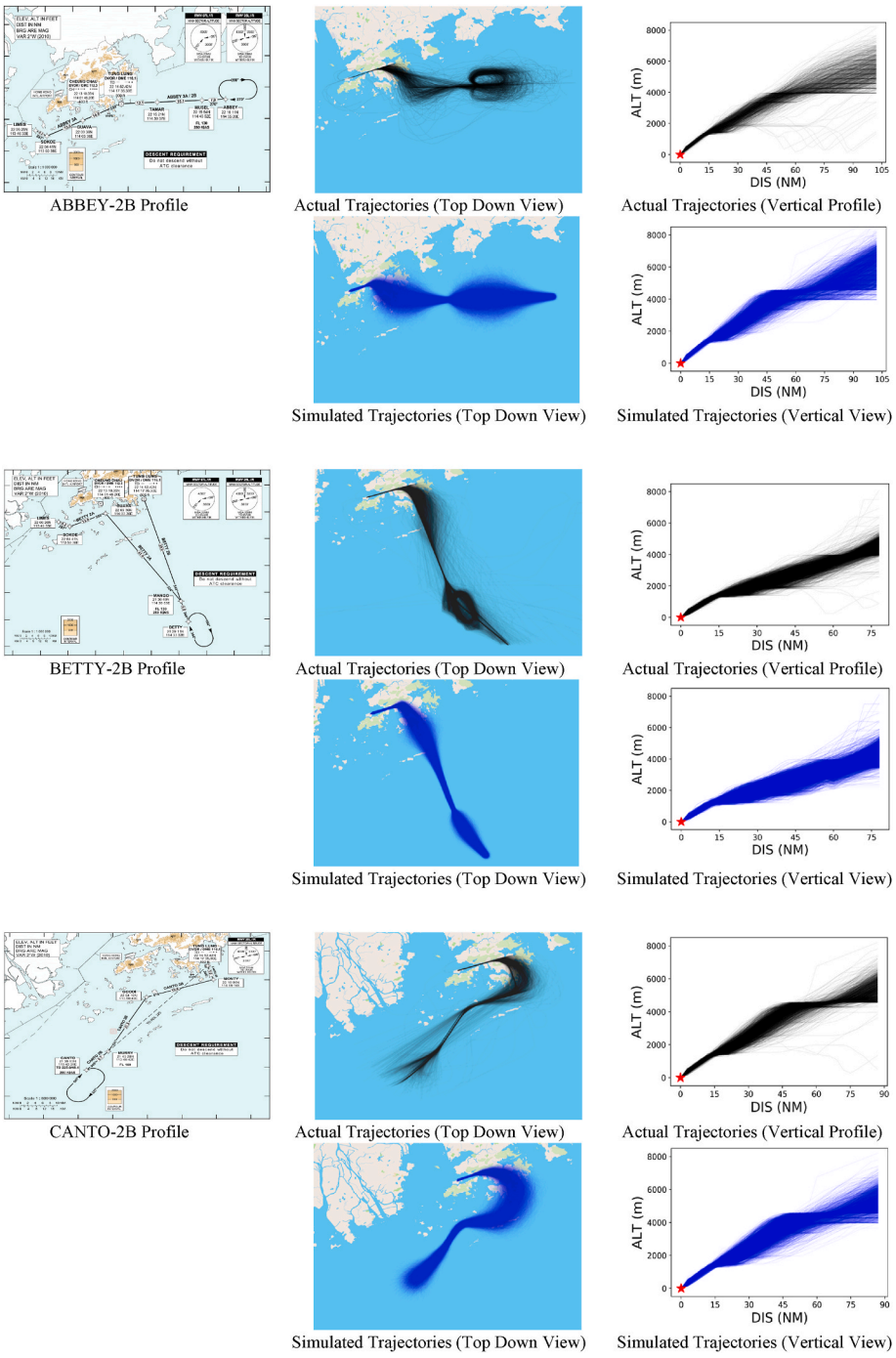

Fig. 14. Training set: ABBEY-2B, BETTY-2B, and CANTO-2B.

STARs and test it on the fourth STAR as depicted in Fig. 13 and Table 7, to simulate the situation when given a new or redesigned STAR profile in current terminal airspace.

3. Evaluation and Testing of MLPNN

To compare with MLPNN, we tested three other regression methods: 1) the RF method, which is suitable for complicated tasks, owing to its capacity in handling big data with numerous variables running into thousands (Genuer et al., 2017); 2) the SVR method, a kernel-based technique (Awad and Khanna, 2015); 3) the GPR method, which has internal structure to capture uncertainties in predictions (Boyle and Frean, 2005).

The metrics used to evaluate the models is the prediction accuracy (PA), which is defined to be calculated by the formula,

$$PA = 100\% - MAPE \tag{10}$$

where MAPE is the abbreviation of commonly used metrics mean absolute percentage error, and it is defined by the formula,

$$MAPE = \frac{100\%}{n} \sum_{i=1}^{n} \left| \frac{A_i - F_i}{A_i} \right| \tag{11}$$

where A_i is the actual value and F_i is the forecast value. The models with high PA values are preferred.

Table 8 and Table 9 report the parameter settings for the MLPNN

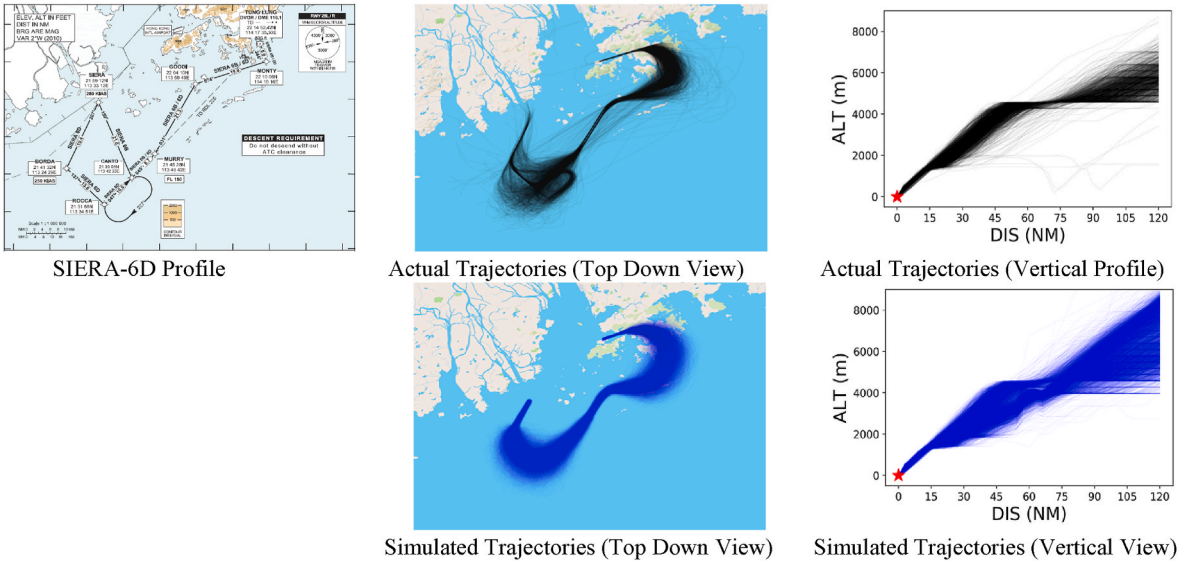

Fig. 15. Testing set: SIERA-6D.

Table 11
Fuel burn in terminal airspace estimation results.

Fuel Consumption	Mean Value	Median Value
FDR Data	1136.8 kg	1149 kg
Simulation Data	1126.5 kg	1113.2 kg
Estimation Accuracy	**99.10%**	**96.90%**

model, and the other four models, respectively. For the RF model training, the number of trees was set to 100. For SVR and GPR models training, the Gaussian radial basis function (RBF) kernel was used and defined as $(S_1, S_2) = exp\left(-\frac{\|S_1 - S_2\|^2}{2\sigma^2}\right)$, where S_1 and S_2 are two points and σ' is the kernel hyper-parameter. For GPR models, the kernel's hyper-parameters are optimized during fitting based on the 'L-BFGS-B' algorithm (Zhu et al., 1997). All the parameters in these models are optimized based on grid search and selected in the predefined ranges, and the best combination is selected according to the criterion, mean squared error (MSE) or root-mean-square error (RMSE).

The performances of the RF, SVR, GPR and MLPNN models trained by the processed ADS-B data are summarized in Table 10. We found that MLPNN performed significantly better, and was more accurate by 3% on average than the other four models. The estimation accuracy of MLPNN could achieve 87.43% on average, implying that the relationship between the features extracted and the designed output variables is well built for trajectory generation.

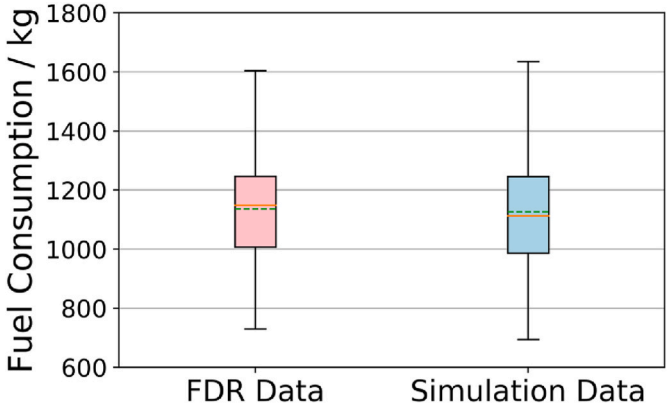

Fig. 16. Boxplots of fuel burn estimation results by the MLPNN.

5. Trajectory generation in Hong Kong airspace

We simulate trajectories for arrival procedure design SIERA-6D based on the MLPNN module using Gaussian distribution and exponential moving average algorithms.

First, we do the trajectory reconstruction and feature engineering for the STAR, SIERA-6D. Next, the five standard variations are predicted from the developed MLPNN model. For the data point i in SIERA-6D, we have the mean $\mu_i = (X_i, Y_i, Z_i, V_{hi}, V_{vi})$ and the standard deviations $\sigma_i = (\sigma_{Xi}, \sigma_{Yi}, \sigma_{Zi}, \sigma_{GSi}, \sigma_{VSi})$. Based on the assumptions and the PDFs illustrated in Section 2.3, we create five normally distributed sets of random numbers of $(X_i^{'}, Y_i^{'}, Z_i^{'}, V_h^{'}i, V_v^{'}i)$ for each data point and then generate new trajectories by making connections of these simulated points $(X_i^{'}, Y_i^{'}, Z_i^{'})$ in order of data point sequencing number i. Then, trajectory smoothing is conducted by applying the EMA algorithm with the smoothing factor β set to 0.3. In this study, we simulated 10,000 new trajectories.

In this study, we focus on the designated flying ranges for different STARs: (1) for ABBEY-2B, the range of study is from waypoint ABBEY to the threshold of the runway; (2) for BETTY-2B, the range is from waypoint BETTY to the threshold of the runway; (3) for CANTO-2B, the range is from waypoint CANTO to the threshold of the runway; (4) for SIERA-6D, the range is from waypoint SIERA to the threshold of the runway.

The comparisons of the published arrival procedures, the actual trajectories, and the simulated trajectories from the proposed model, are shown in Fig. 14 for training sets and Fig. 15 for testing on SIERA-6D. The results show that even the model is trained on ABBEY-2B, BETTY-2B, and CANTO-2B, it can simulate trajectories for SIERA-6D and show

Table 12
Actual fuel burn compared with ideal fuel burn in terminal airspace.

	ABBEY-2B	BETTY-2B	CANTO-2B	SIERA-6D
Ideal Fuel Burn (kg)	600.0	700.0	700.0	900.0
Actual Fuel Burn (Mean) (kg)	823.6	917.9	863.2	1136.8
Over Consumption (kg)	223.6	217.9	163.2	236.8
Percentage of Over Consumed (%)	37.3	31.1	23.3	26.3
Estimated Fuel Burn (kg)	835.1	901.4	847.6	1126.5
Estimation Accuracy (%)	98.6	98.2	98.2	99.1

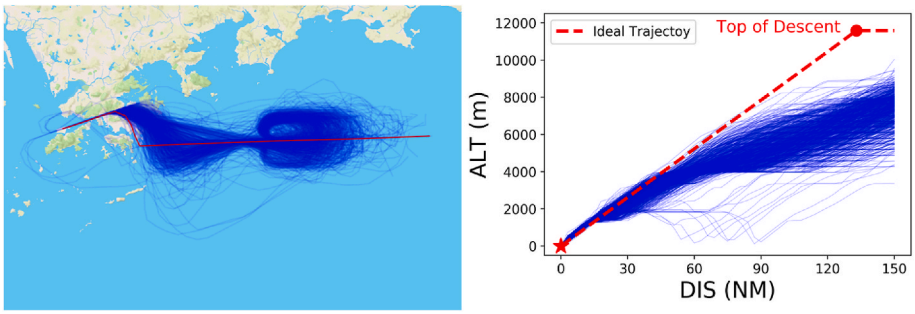

Horizontal and vertical plots for ABBEY-2B

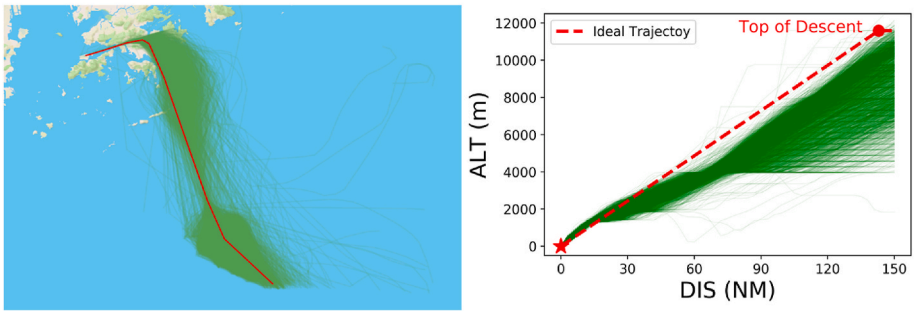

Horizontal and vertical plots for BETTY-2B

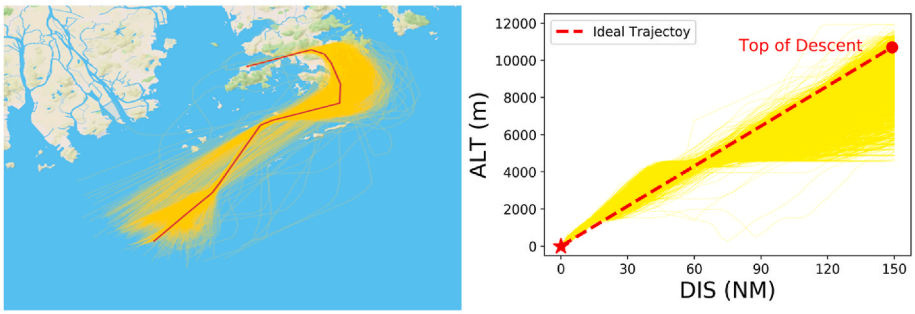

Horizontal and vertical plots for CANTO-2B

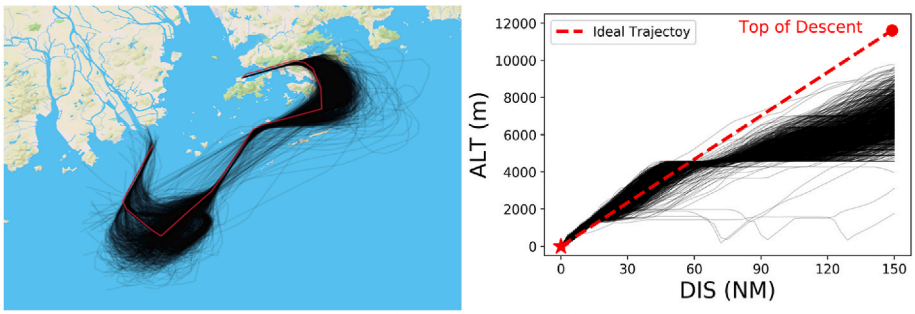

Horizontal and vertical plots for SIERA-6D

Fig. 17. Actual trajectory compared with the ideal trajectory in Hong Kong terminal airspace.

high similarity compared with the actual trajectories.

5. Fuel Consumption Estimation and Analysis

In this part, we evaluate the arrival procedure SIERA-6D of Hong Kong terminal airspace from the perspective of fuel efficiency, using a fuel consumption estimation model developed by Hong and Li (N. Hong and Li, 2018). This fuel consumption estimation model was trained based on the Digital Flight Data Recorder (FDR) data of 2686 flights landing at HKIA during November in 2014, and from April to June in 2015. As shown in Fig. 8, the inputs of the fuel consumption estimation model are the aircraft altitude, the air temperature, the calibrated airspeed, flying distance, and the aircraft mass when descending. The outputs are the average fuel burn in the terminal area when flying in SIERA-6D designs. The prediction accuracy of the fuel consumption estimation model is 96.6% on average. The detailed information about the fuel consumption estimation model training process can be found in (N. Hong and Li, 2018).

Feeding the simulated trajectories of SIERA-6D into the fuel consumption model, we obtain the fuel burn if SIERA-6D were flew. Compared with the actual fuel consumption from the FDR data, the fuel consumption of the simulated trajectories is in agreement, as shown in Table 11 and Fig. 16.

To further demonstrate the value of generating trajectories

considering uncertainties, we analyze the difference between the ideal fuel burn if aircraft could follow STAR precisely and the fuel burn in practice. The results are shown in Table 12. When flying SIERA-6D, the ideal fuel burn is 900 kg if the aircraft could fly exactly as the designed procedure from waypoint SIERA to the threshold of the runway. This reference number is obtained from an airline's flight planning system. The actual fuel burn obtained from FDR data is more than 1100 kg, which indicates that the current operations of SIERA-6D in Hong Kong airspace are not fuel-efficient. Similar analyses are conducted for four STARs. Compared with the ideal fuel consumption values, the actual fuel consumption is 37.27%, 31.13%, 23.31% and 26.31% more on average for ABBEY-2B, BETTY-2B, CANTO-2B and SIERA-6B/6D, respectively. Fig. 17 shows the flight profiles of the actual operations compared with the ideal ones (highlighted in red). Currently, aircraft fly much lower than the planned profiles, which is a major factor that causes the fuel over-consumption of flights that arrive at Hong Kong airport. If the proposed trajectory generation model was used, similar numbers can be obtained via a fast system-level simulation approach without requiring the FDR data.

6. Conclusion

In this research, we developed a novel trajectory generation model based on MLPNN, which predicts aircraft trajectories with uncertainties for airspace redesign analysis. The proposed framework included three parts: 1) input-and-output construction, 2) supervised learning via MLPNN, and 3) trajectory generation. Trajectory reconstruction of operational data, feature engineering, and output designing for supervised learning were performed first. Next, the MLPNN was built to predict the relationship between the standard deviations and extracted features. Finally, the trajectories with uncertainties were simulated by applying Gaussian distribution and EMA algorithms.

The proposed framework was evaluated and tested on ADS-B data in Hong Kong terminal airspace. We found that the MLPNN model achieved good prediction performance and it was better than other machine learning methods based on RF, SVR, and GPR, respectively. We also demonstrated the usage of the proposed framework in estimating the real fuel consumption, to evaluate current STAR designs from the perspective of fuel efficiency in Hong Kong terminal airspace. In addition, our proposed framework can be adapted to evaluate standard procedures in other terminal airspaces.

However, in this model, the shape of simulated trajectories is closely linked to the probability distribution functions assumed. In this research, we assume that simulated trajectories follow Gaussian distribution; however, it may not hold for some special segments of the trajectories in real operations. For example, the current model cannot capture the characteristics of holding patterns. Besides, we only considered the diagonal variance estimation of Gaussian while ignoring the prediction of covariance, which will be further investigated. Other distribution assumptions will have potential to improve the Gaussian assumption such as truncated Gaussians could be applied when defining the normal range and would like to investigate the possibility of extreme values outside the range. Normalizing flow will be another worthy direction to assume the distribution since it can model the underlying complex probabilistic distributions. Dynamical system approach could be another direction to explore.

Future work is planned to focus on two parts, 1) improvement on the feature engineering part to capture special patterns of the flight routes, such as the holding pattern, 2) extension of the proposed model to trajectory generation of other types of vehicles, such as unmanned aerial vehicles, freighters, maritime vessels cars, etc.

Author statement

Xinting Zhu: Methodology, Software, Writing- Reviewing and Editing; **Ning Hong:** Methodology, Visualization, Writing- Original draft preparation; **Fang He:** Data curation, Investigation; **Yu Lin:** Software, Validation; **Lishuai Li:** Conceptualization, Supervision, Project administration, Funding acquisition; **Xiaowen Fu:** Supervision.

Data availability

The data that has been used is confidential.

Acknowledgment

The work was supported by the Hong Kong Research Grants Council General Research Fund (Project No. 11215119 and 11209717), ITF - Guangdong-Hong Kong Technology Cooperation Funding Scheme (Ref. No. GHP/145/20), and CityU Strategic Interdisciplinary Research Grant (Project Ref. No. 2022SIRG035).

References

Airport Authority Hong Kong, 2011. Three-runway system | three runway system. https://www.threerunwaysystem.com/en/.

Alligier, R., Gianazza, D., Durand, N., 2015. Machine learning and mass estimation methods for ground-based aircraft climb prediction. IEEE Trans. Intell. Transport. Syst. 16 (6), 3138–3149. https://doi.org/10.1109/TITS.2015.2437452.

Awad, M., Khanna, R., 2015. Support vector regression. In: Awad, M., Khanna, R. (Eds.), Efficient Learning Machines: Theories, Concepts, and Applications for Engineers and System Designers, pp. 67–80. https://doi.org/10.1007/978-1-4302-5990-9_4. Apress.

Ayhan, S., Samet, H., 2016. Aircraft trajectory prediction made easy with predictive analytics. In: Proceedings of the 22nd ACM SIGKDD International Conference on Knowledge Discovery and Data Mining, pp. 21–30. https://doi.org/10.1145/2939672.2939694.

Barratt, S.T., Kochenderfer, M.J., Boyd, S.P., 2018. Learning probabilistic trajectory models of aircraft in terminal airspace from position data. IEEE Trans. Intell. Transport. Syst. 1–10. https://doi.org/10.1109/TITS.2018.2877572.

Bilimoria, K.D., Sridhar, B., Grabbe, S.R., Chatterji, G.B., Sheth, K.S., 2001. FACET: future ATM concepts evaluation tool. Air Traffic Control Q 9 (1). https://doi.org/10.2514/atcq.9.1.1.

Boeing Commercial Airplanes, 2020. Statistical Summary of Commercial Jet Airplane Accidents: World Wide Operations 1959–2019.

Bongiorno, C., Gurtner, G., Lillo, F., Mantegna, R.N., Miccichè, S., 2017. Statistical characterization of deviations from planned flight trajectories in air traffic management. J. Air Transport. Manag. 58, 152–163. https://doi.org/10.1016/j.jairtraman.2016.10.009.

Boyle, P., Frean, M., 2005. Dependent Gaussian processes. In: Saul, L.K., Weiss, Y., Bottou, L. (Eds.), Advances in Neural Information Processing Systems, 17. MIT Press, pp. 217–224.

Chazal, F., Chen, D., Guibas, L., Jiang, X., Sommer, C., 2011. Data-driven Trajectory Smoothing, p. 251. https://doi.org/10.1145/2093973.2094007.

CSSI Inc. (n.d.). Terminal Area Route Generation, Evaluation and Traffic Simulation Software Brochure. Retrieved September 27, 2021, from https://targets.cssiinc.com/external/downloads/documents/TARGETS-Brochure.pdf.

de Leege, A.M.P., van Paassen, M.M., Mulder, M., 2013. A machine learning approach to trajectory prediction. In: AIAA Guidance, Navigation, and Control (GNC) Conference. https://doi.org/10.2514/6.2013-4782.

Gariel, M., Srivastava, A.N., Feron, E., 2011. Trajectory clustering and an application to airspace monitoring. Intelligent Transportation Systems, IEEE Transactions On 12 (4), 1511–1524.

Genuer, R., Poggi, J.-M., Tuleau-Malot, C., Villa-Vialaneix, N., 2017. Random forests for big data. Big Data Research 9, 28–46. https://doi.org/10.1016/j.bdr.2017.07.003.

Hamed, M.G., Gianazza, D., Serrurier, M., Durand, N., 2013. Statistical Prediction of Aircraft Trajectory: Regression Methods vs Point-Mass Model. 10th USA/Europe Air Traffic Management Research and Developpment Seminar. *ATM 2013)*.

Hong, N., Li, L., 2018. A data-driven fuel consumption estimation model for airspace redesign analysis. In: 2018 IEEE/AIAA 37th Digital Avionics Systems Conference (DASC), pp. 1–8. https://doi.org/10.1109/DASC.2018.8569564.

Hong, S., Lee, K., 2015. Trajectory prediction for vectored area navigation arrivals. J. Aero. Inf. Syst. 12 (7), 490–502. https://doi.org/10.2514/1.I010245.

Huang, H., Tomlin, C., 2009. A network-based approach to en-route sector aircraft trajectory planning. In: AIAA Guidance, Navigation, and Control Conference. https://doi.org/10.2514/6.2009-6169.

Jarry, G., Delahaye, D., Nicol, F., Feron, E., 2020. Aircraft atypical approach detection using functional principal component analysis. J. Air Transport. Manag. 84, 101787 https://doi.org/10.1016/j.jairtraman.2020.101787.

Jilkov, V.P., Ledet, J.H., Li, X.R., 2019. Multiple model method for aircraft conflict detection and resolution in intent and weather uncertainty. IEEE Trans. Aero. Electron. Syst. 55 (2), 1004–1020. https://doi.org/10.1109/TAES.2018.2867698.

Khan, W.A., Ma, H.L., Ouyang, X., Mo, D.Y., 2021. Prediction of aircraft trajectory and the associated fuel consumption using covariance bidirectional extreme learning machines. Transport. Res. E Logist. Transport. Rev. 145, 102189 https://doi.org/10.1016/J.TRE.2020.102189.

Li, M.Z., Ryerson, M.S., 2017. A data-driven approach to modeling high-density terminal areas: a scenario analysis of the new Beijing, China airspace. Chin. J. Aeronaut. 30 (2), 538–553. https://doi.org/10.1016/j.cja.2016.12.030.

Li, M.Z., Suh, D.Y., Ryerson, M.S., 2018. Visualizing aviation impacts: modeling current and future flight trajectories with publicly available flight data. Transport. Res. Transport Environ. 63, 769–785. https://doi.org/10.1016/j.trd.2018.07.009.

Li, T., Wan, Y., 2021. A fuel savings and benefit analysis of reducing separation standards in the oceanic airspace managed by the New York Air Route Traffic Control Center. Transport. Res. E Logist. Transport. Rev. 152, 102407 https://doi.org/10.1016/J.TRE.2021.102407.

Liu, W., Hwang, I., 2011. Probabilistic trajectory prediction and conflict detection for air traffic control. J. Guid. Control Dynam. 34, 1779–1789. https://doi.org/10.2514/1.53645.

Lymperopoulos, I., Lygeros, J., 2010. Sequential Monte Carlo methods for multi-aircraft trajectory prediction in air traffic management. Int. J. Adapt. Control Signal Process. 24 (10), 830–849. https://doi.org/10.1002/acs.1174.

Mahboubi, Z., Kochenderfer, M.J., 2017. Learning traffic patterns at small airports from flight tracks. IEEE Trans. Intell. Transport. Syst. 18 (4), 917–926. https://doi.org/10.1109/TITS.2016.2598064.

Marzuoli, A., Gariel, M., Vela, A., Feron, E., 2014. Data-based modeling and optimization of en route traffic. J. Guid. Control Dynam. 37 (6), 1930–1945. https://doi.org/10.2514/1.G000010.

MITRE, 2021. Terminal Area Route Generation and Traffic Simulation (TARGETS). https://www.mitre.org/research/technology-transfer/technology-licensing/terminal-area-route-generation-and-traffic.

Murça, M.C.R., Guterres, M.X., de Oliveira, M., Tarelho Szenczuk, J.B., Souza, W.S.S., 2020. Characterizing the Brazilian airspace structure and air traffic performance via trajectory data analytics. J. Air Transport. Manag. 85, 101798 https://doi.org/10.1016/j.jairtraman.2020.101798.

Murca, M.C.R., Hansman, R.J., 2019. Identification, characterization, and prediction of traffic flow patterns in multi-airport systems. IEEE Trans. Intell. Transport. Syst. 20 (5), 1683–1696. https://doi.org/10.1109/TITS.2018.2833452.

Murça, M.C.R., Müller, C., 2015. Control-based optimization approach for aircraft scheduling in a terminal area with alternative arrival routes. Transport. Res. E Logist. Transport. Rev. 73, 96–113. https://doi.org/10.1016/J.TRE.2014.11.004.

Nair, V., Hinton, G.E., 2010. Rectified linear units improve restricted Boltzmann machines. In: Proceedings of the 27th International Conference on Machine Learning (ICML-10).

Olive, X., Morio, J., 2019. Trajectory clustering of air traffic flows around airports. Aero. Sci. Technol. 84, 776–781. https://doi.org/10.1016/J.AST.2018.11.031.

Pfeil, D.M., 2011. Optimization of Airport Terminal-Area Air Traffic Operations under Uncertain Weather Conditions. Massachusetts Institute of Technology.

Ren, P., Li, L., 2018. Characterizing air traffic networks via large-scale aircraft tracking data: a comparison between China and the US networks. J. Air Transport. Manag. 67, 181–196. https://doi.org/10.1016/j.jairtraman.2017.12.005.

Rosenow, J., Fricke, H., 2019. Impact of multi-criteria optimized trajectories on European airline efficiency, safety and airspace demand. J. Air Transport. Manag. 78, 133–143. https://doi.org/10.1016/j.jairtraman.2019.01.001.

Seah, C.E., Hwang, I., 2009. Terminal-area aircraft tracking using hybrid estimation. J. Guid. Control Dynam. 32 (3), 836–849. https://doi.org/10.2514/1.40127.

Sidiropoulos, S., Majumdar, A., Han, K., 2018. A framework for the optimization of terminal airspace operations in Multi-Airport Systems. Transp. Res. Part B Methodol. 110, 160–187. https://doi.org/10.1016/j.trb.2018.02.010.

Tastambekov, K., Puechmorel, S., Delahaye, D., Rabut, C., 2014. Aircraft trajectory forecasting using local functional regression in Sobolev space. Transport. Res. C Emerg. Technol. 39, 1–22. https://doi.org/10.1016/j.trc.2013.11.013.

Tomlin, C., Pappas, G.J., Sastry, S., 1998. Conflict resolution for air traffic management: a study in multiagent hybrid systems. IEEE Trans. Automat. Control 43 (4), 509–521. https://doi.org/10.1109/9.664154.

Visintini, A.L., Glover, W., Lygeros, J., Maciejowski, J., 2006. Monte Carlo optimization for conflict resolution in air traffic control. IEEE Trans. Intell. Transport. Syst. 7 (4), 470–482. https://doi.org/10.1109/TITS.2006.883108.

Wang, Z., Liang, M., Delahaye, D., 2018. A hybrid machine learning model for short-term estimated time of arrival prediction in terminal manoeuvring area. Transport. Res. C Emerg. Technol. 95, 280–294. https://doi.org/10.1016/j.trc.2018.07.019.

Yepes, J.L., Hwang, I., Rotea, M., 2007. New algorithms for aircraft intent inference and trajectory prediction. J. Guid. Control Dynam. 30 (2), 370–382. https://doi.org/10.2514/1.26750.

Zhou, J., Cafieri, S., Delahaye, D., Sbihi, M., 2014. Optimization of arrival and departure routes in terminal maneuvering area. In: ICRAT 2014, 6th International Conference on Research in Air Transportation.

Zhu, C., Byrd, R.H., Lu, P., Nocedal, J., 1997. Algorithm 778: l-BFGS-B: fortran subroutines for large-scale bound-constrained optimization. ACM Trans. Math Software 23 (4), 550–560. https://doi.org/10.1145/279232.279236.